

perform better than the  $\sqrt{L+1}$  active correlator serial search at the SNRs of interest.

The results of this analysis are the estimated hardware complexity and acquisition time of the C/F approach as compared with the full symbol match filter alternative. The hardware complexity of the C/F approach is less than the match filter for two reasons. First, storage requirements are significantly reduced because a full symbol of data need not be stored to compute each test statistic. Second, the number of computational elements is reduced because the total number of correlations computed for each symbol is reduced from  $L$  to  $\sqrt{L+1}$ . This leads to a significant savings in the cost of implementing digital correlators for large code lengths.

ADAM C. VON ANCKEN  
RONALD D. WILLIAMS  
MAXIMO H. SALINAS  
Department of Electrical Engineering  
Thornton Hall  
University of Virginia  
Charlottesville, VA 22903-2442

#### REFERENCES

- [1] Chawla, K. K., and Sarwate, D. V. (1994)  
Parallel acquisition of PN sequences in DS/SS systems.  
*IEEE Transactions on Communications*, **42**, 5 (May 1994),  
2155–2164.
- [2] Su, Y. T. (1988)  
Rapid code acquisition algorithms employing PN matched  
filters.  
*IEEE Transactions on Communications*, **36**, 6 (June 1988),  
724–733.
- [3] Madhow, U., and Pursley, M. B. (1995)  
Mathematical modeling and performance analysis for  
a two-stage acquisition scheme for direct-sequence  
spread-spectrum CDMA.  
*IEEE Transactions on Communications*, **43**, 9 (Sept. 1995),  
2511–2520.
- [4] Holmes, J. K. (1982)  
*Coherent Spread Spectrum Systems*.  
New York: Wiley, 1982.

## Receiver Antenna Scan Rate Requirements Needed to Implement Pulse Chasing in a Bistatic Radar Receiver

Pulse chasing is a technique implemented by a bistatic or multistatic radar system that allows rapid and efficient search of a desired volume of space whereby the receiving antenna is made to follow or “chase” the transmitted pulse as it travels radially outward from the transmitter antenna. An expression for receiver antenna scan rate requirements is derived that corrects an error in the prior literature. The results give significantly reduced scan rates in the forward scatter region near the baseline showing that pulse chasing is more easily implemented using conventional analog beamformer phased array technology than was suggested by prior work.

### I. INTRODUCTION

A bistatic or multistatic radar is defined as a radar having different transmitting and receiving antennas which are in general not collocated [1–3]. The bistatic radar system geometry provided in Fig. 1 shows the

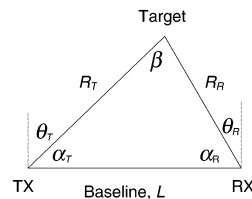


Fig. 1. Bistatic radar geometry.

bistatic triangle having sides  $R_T$ ,  $R_R$ , and  $L$ . In the literature  $L$  is referred to as the *baseline* length, and the bistatic angle  $\beta$  is defined as the angle subtended between the transmitter to target and receiver to target directions. References [1–3] give transmitter and receiver angles  $\theta_R$  and  $\theta_T$ , respectively, however this paper uses transmitter and receiver angles  $\alpha_R$  and  $\alpha_T$  as defined in Fig. 1. The forward scatter region is the area in the general vicinity between the transmitter and receiver, or likewise, where the bistatic angle is about  $180^\circ$ .

Manuscript received September 12, 1998; revised September 5, 1999, February 26 and September 29, 2000; released for publication October 2, 2000.

IEEE Log No. T-AES/37/1/02935.

Refereeing of this contribution was handled by W. D. Blair.

U.S. Government work not protected by U.S. copyright.

0018-9251/01/\$10.00 IEEE

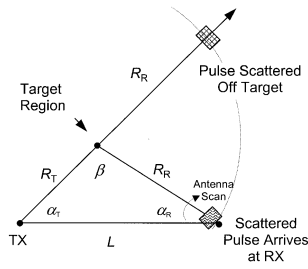


Fig. 2. Illustration of bistatic radar system employing pulse chasing technique. Energy scattered from target arrives at receiver just as RX antenna is pointed to angle  $\alpha_R$ . TX, RC, and target form resulting triangle to be solved.

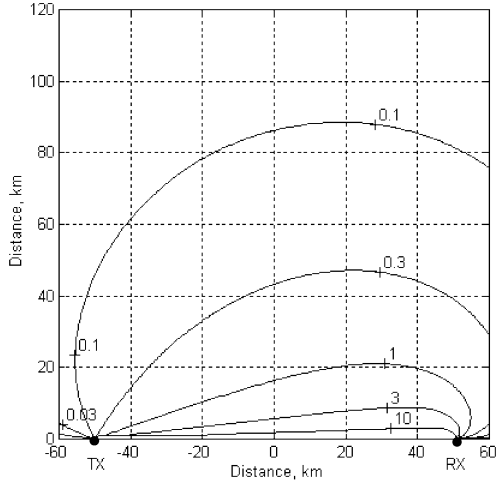


Fig. 3. Receiver antenna scan rate requirements for  $L = 100$  km computed as shown in [1, Fig. 14]. Contour units are degrees per microsecond.

Pulse chasing is a bistatic radar technique used for efficiently searching a volume of space whereby the receive beam is made to lock onto the transmitted pulse and follow it as it radiates outward from the transmitter, as illustrated in Fig. 2. Of particular interest to the radar designer are the scan rate requirements needed for the receiving antenna, which is usually implemented with an electronically steered antenna such as a phased array antenna. A method for computing the scan rate is given by<sup>1</sup> [1–3]

$$\dot{\theta}_R = \frac{c}{R_R} \tan(\beta/2) \quad (1)$$

where  $c$  is the velocity of light ( $c \approx 3 \times 10^8$  m/s). Fig. 3 shows an iso-scan rate contour plot of (1) with units of degrees per microsecond, for a baseline of  $L = 100$  km.

The method given by (1) suggests that the scan rate is dependent on only two parameters; side  $R_R$ , and angle  $\beta$ , and is not dependent on a third parameter such as the baseline distance  $L$ . This point is discussed further in Section II. The method in (1) further states that in the forward scatter region, when  $\beta \rightarrow 180^\circ$  the scan rate requirement increases

<sup>1</sup>This was originally formulated in [1] and later published in [2, 3].

without bound. However the condition that occurs as  $\beta \rightarrow 180^\circ$  is when the transmit and receive antenna are directly pointed at each other and the target region lies directly between the transmit and receiver. Under this condition the receiver antenna is pointed at the transmitter and must remain stationary when implementing pulse chasing. Therefore when  $\beta \rightarrow 180^\circ$  the receiver antenna is not needed to scan and hence the scan rate should be zero. This condition is in conflict with the above expression (1) for scan rate. The derivation provided herein corrects this error [4].

## II. ANALYSIS

The bistatic pulse chasing technique as illustrated in Fig. 2 requires the antenna to appropriately lock on and track the transmitted pulse so that energy scattered from the target arrives at the receiver antenna. If a pulse is emitted from the transmitter at time  $t' = 0$ , then energy will just arrive at the receiver subject to a delay equal to the time required for the pulse to travel from the transmitter to receiver antenna,  $t' = L/c$ . Therefore for the receiver point of view the receiver antenna must just begin to scan at a time  $t = 0$  delayed by  $L/c$  after the pulse has been transmitted.

When the receiver antenna is pointed to angle  $\alpha_R$  at time  $t \geq 0$  the receiver antenna will capture energy from the target region located at a distance of  $ct$  from the transmitter. Then from Fig. 2 the distance from the transmitter to the target region searched is therefore

$$R_T = c(t' - L/c) = ct \quad (2)$$

valid for  $t' \geq L/c$  or equivalently  $t \geq 0$ . By inspection of Fig. 2 the target, receiver and transmitter will form a triangle having the sides  $L$ ,  $R_R$ ,  $R_T$  and angles  $\beta$ ,  $\alpha_R$ , and  $\alpha_T$ , each which can be expressed either as constants or as a function of time during one pulse chase scan period. The side  $L$  and angle  $\alpha_T$  are constants with respect to time since the position of the transmitter antenna remains fixed and the pulse will propagate in a fixed direction once transmitted. The remaining sides and angles will vary as function of time and specifically the time derivative of  $\alpha_R$  will be solved to determine the receiver antenna scan rate required to implement pulse chasing. Considering the bistatic triangle in Fig. 2, from the law of sines

$$\frac{R_R}{\sin \alpha_T} = \frac{R_T}{\sin \alpha_R} = \frac{L}{\sin \beta}. \quad (3)$$

By inspection one obtains

$$L = R_T \cos \alpha_T + R_R \cos \alpha_R. \quad (4)$$

Substituting (2) and (3) into (4) one obtains angle  $\alpha_R$  as a function of time given by

$$\alpha_R(t) = \cot^{-1} \left[ \frac{L - ct \cos \alpha_T}{ct \sin \alpha_T} \right] \quad (5)$$

valid for  $t > 0$  and  $\alpha_T \neq 0, 180^\circ$ .

Equation (5) is considered for the general bistatic case with the bistatic triangle. Since angles  $\alpha_R$  and  $\theta_R$  differ only by a constant, the time derivatives of these two angles are also the same to within a sign. Therefore the scan rate required to implement pulse chasing is given by  $\dot{\alpha}_R = -\dot{\theta}_R$ .

Noting that (5) is of the form  $\cot^{-1}(u)$  where  $u = (L - ct \cos \alpha_T)/ct \sin \alpha_T$  the time derivative is found to be of the form

$$\dot{\alpha}_R = \frac{d}{dt}[\cot^{-1}(u)] = -\frac{1}{1+u^2} \frac{du}{dt} \quad (6)$$

which simplifies to

$$\dot{\theta}_R = \frac{cL \sin \alpha_T}{(ct \sin \alpha_T)^2 + (L - ct \cos \alpha_T)^2}. \quad (7)$$

A useful result is obtained by substituting (2) into (7) and the scan rate can be expressed as

$$\dot{\theta}_R = \frac{17.2L \sin \alpha_T}{(R_T \sin \alpha_T)^2 + (L - R_T \cos \alpha_T)^2} \text{ [degrees/microsecond]} \quad (8)$$

where  $L$  and  $R_T$  are in units of kilometers. The scan rate given by (8) is a function of  $\beta$  as given implicitly by (3). It is also noted in the results of (2)–(8) that scan rate can be expressed as a function of sides  $L$ ,  $ct = R_T$  and angle  $\alpha_T$ . The results are therefore expressed using a combination of three sides and angles of the bistatic triangle. This result is obtained because specification of *three* parameters (any combination of 1) two sides and one angle, or 2) one side and two angles, or 3) three sides) are necessary and sufficient to solve a general triangle. The result derived above is in contrast to the work from prior literature [1–3] in (1) which essentially states that the scan rate can be solved with knowledge of only *two* parameters of the triangle including side  $R_R$ , and angle  $\beta$ , which are insufficient conditions for specifying a general triangle.

### III. SUMMARY OF RESULTS

An examination of the derived results is now provided. A contour plot of scan rate  $\dot{\theta}_R$  given by (8) is shown in Fig. 4 for baseline of 100 km. The figure shows the scan rates needed in both the backscatter and forward scatter regions along the baseline. Fig. 4 clearly indicates some basic differences when compared with Fig. 3 computed with (1). By evaluation of (8) and from comparison of Figs. 3 and 4 the following general observations are made.

1) When the bistatic angle  $\beta \rightarrow 180^\circ$  or likewise  $\alpha_R \approx \alpha_T \rightarrow 0$  (i.e., forward scatter along the baseline), the scanning rate is zero. The scan rate must equal zero under this condition since both the transmit and receive antennas are pointing toward each other. This

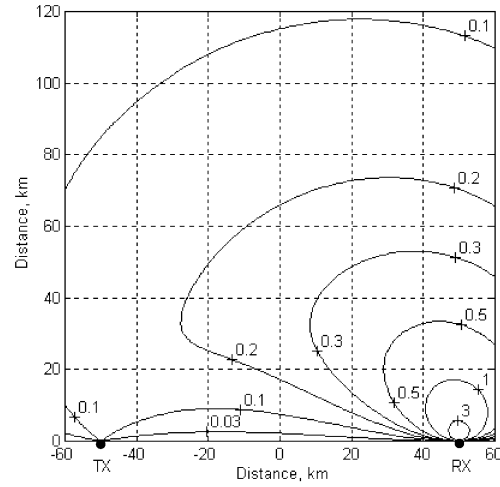


Fig. 4. Receiver antenna scan rate requirements for  $L = 100$  km computed using proposed technique given by (8). Contour units are degrees per microsecond.

is in contrast with (1), which shows the scan rate increasing without bound.

2) As the distance from the target to the receiver is decreased, the scan rate tends to increase. Very near the receiver at roughly normal to the baseline, the scan rate becomes prohibitively large (by inspection of the denominator of (8) this occurs when  $\alpha_T \approx 0$  and  $L \approx R_T \cos \alpha_T$ ). This may restrict the use of pulse chasing in the region very near the receiver, except for the special case along the baseline ( $\beta \approx 180^\circ$ ).

3) The scan rate is a function of the baseline distance  $L$ . This is in contrast to the method given in (1) which suggests the scan rate can be expressed without specifying  $L$ . The difference in the two methods of (1) and (8) is due to that fact that (1) does not completely specify the triangle which defines the bistatic geometry whereas (8) does, as discussed in Sections I and II.

4) Digital beamforming (DBF) array methods are commonly employed in bistatic receiver systems [5, 6]. DBF techniques use an array of antenna elements and analog-to-digital (A/D) converters which operate in the receive mode and perform post processing to search for targets within the received, sampled signal. The results derived here show that the scan rate is “well behaved” in the forward scatter region and therefore more achievable using conventional phase shifter antenna technology (e.g., diode phase shifters) than was suggested in prior literature [1–3]. One need not consider only DBF for bistatic receivers but may also consider electronically scanned arrays using conventional (analog) beamforming as well.

### ACKNOWLEDGMENTS

The author wishes to express his appreciation for the thoughtful and helpful suggestions of the reviewers.

## REFERENCES

- [1] Jackson, M. C. (1986)  
The geometry of bistatic radar systems.  
*IEEE Proceedings*, **133**, pt. F (Dec. 1986), 604–612.
- [2] Willis, N. J. (1991)  
*Bistatic Radar*.  
Norwood, MA: Artech House, 1991.
- [3] Skolnik, M. I. (1990)  
*Radar Handbook* (2nd ed.).  
New York: McGraw Hill, 1990.
- [4] Purdy, D. S. (1995)  
A feasibility study of bistatic and multistatic upgrades for the electronic combat range.  
Unpublished report presented to the Electronic Combat Range, Naval Air Warfare Center, China Lake, CA, May, 1995.
- [5] Steyskal, H. (1987)  
Digital beamforming antennas: An introduction.  
*Microwave Journal* (Jan. 1987).
- [6] Fang, M. Y., Wu, M. Q., Wang, Y., Ruan, X., and Huo, R. L. (1997)  
Cumulant-based blind DBF method for an experimental bistatic radar PCBRs-I.  
Radar-97, Publication 449, IEE, 1997.

## Hybrid Power Sources for Pulsed Current Applications

A battery-capacitor hybrid power source was discharged under pulsed current conditions and various ambient temperatures. Significant improvements in voltage drop and run time were obtained with the hybrid device over the battery alone. An equivalent circuit was established to evaluate the voltage behavior of the hybrid device. It was found that at the peak discharge current, as much as 50% of the total energy supplied was provided by a capacitor with only about one-third of the battery's volume.

## INTRODUCTION

Power sources with high-power and high-energy density are urgently needed for a large numbers of portable systems. In many of these applications, including space communications, digital cellular telephones, and electric and hybrid vehicles, the loads are not constant but rather span a range of power

levels. Setting an electrochemical capacitor and a battery side by side constitutes an attractive energy storage system with several distinct advantages, as it exploits both the high-power density of the capacitor and the high-energy density of the battery. The use of an ultracapacitor for improving the pulsed power performance of batteries has already been demonstrated in several examples [1–3]. However, these examples have clearly shown that further improvement in the energy and power density of ultracapacitors is necessary to achieve the maximum potential in high-power applications. Recently high-energy and high-power density ultracapacitors have been developed based on amorphous ruthenium oxide electrodes due to superior specific capacitance (768 F/g) and low electrical resistivity ( $10^{-3} \Omega\text{-cm}$ ) [4, 5].

## DEVICES

A commercially available lithium-ion cell was used as the primary energy source. The battery has a diameter of 2.1 cm, is a height of 5.2 cm, and a total volume of 18 cm<sup>3</sup>. The capacity of the battery is 900 mAh.

An ultracapacitor was made with five cells in series. The electrode was a thin layer coating of (80%) amorphous ruthenium oxide and (20%) carbon, 3.8 cm in diameter on a 5.1 cm diameter conductive polymer film. The thickness of each electrode was about 76  $\mu\text{m}$ , and the electrolyte was 38% sulfuric acid. Five individual cells were clamped together to form a five-cell capacitor, and two 2 mm thick stainless steel plates were used as the end plates and as the current collectors. The ultracapacitor has a 5.3 cm diameter, is 0.35 cm tall, and has a total volume of 6.9 cm<sup>3</sup>. The dc capacitance and internal equivalent series resistance at 1 kHz were 1.0 F and 0.067  $\Omega$ , respectively. The performance of the ultracapacitor was evaluated with a dc charge/discharge test and an ac impedance measurement. For the dc charge/discharge test, the capacitor was charged and discharged at a constant current with a voltage range of 0 to 5 V. A capacitance of 1 F was obtained from the measurement. For the ac impedance measurement, the capacitor was tested over a frequency range of  $10^{-2}$  to  $10^5$  Hz; the equivalent series resistance and capacitance are shown in Fig. 1. It was found that the frequency where the phase is  $-45^\circ$  occurred at about 4 Hz.

For this study, the hybrid device was made by simply connecting the battery and capacitor in parallel without any electronic control in between.

## EXPERIMENTAL RESULTS

The battery and hybrid devices were charged and discharged by a Maccor battery test system. They

Manuscript received February 28, 2000; revised September 12, 2000; released for publication September 29, 2000.

IEEE Log No. T-AES/37/1/02936.

Refereeing of this contribution was handled by W. M. Polivka.

0018-9251/01/\$10.00 © 2001 IEEE